Epitaxial crystallization of linear polyethylene in blends with isotactic polypropylene

F. Rybnikar [a] & M. Kaszonyiova [a]

[a] Department of Production Engineering , Tomas Bata University in Zlin , 760 01 , Czech Republic
Accepted author version posted online: 29 Jul 2013.

Epitaxial crystallization of linear polyethylene in blends with isotactic polypropylene

Rybnikar F., Kaszonyiova M.

Department of Production Engineering, Tomas Bata University in Zlin, 760 01, Czech Republic

*for correspondence, e-mail: mhribova@ft.utb.cz

Abstract

The structure and morphology of extrusion oriented ribbons of polypropylene / polyethylene blends is described. The blends with 20, 30 and 40% of oriented isotactic polypropylene fibrils show homo- and hetero- epitaxial structures. Partial mutual solubility of the blend components influenced the melting and crystallization behavior.

Keywords: linear polyethylene, isotactic polypropylene blends, homo-epitaxy, hetero-epitaxy, blend melting, crystallization

INTRODUCTION

Heterogeneous epitaxial crystallization, as a specific nucleation event between different polymer or substrate pairs, is still attracting much attention [1-7], especially for incompatible polymer systems [8,9]. E.g., linear polyethylene (LPE) and isotactic polypropylene (iPP) blends have been investigated intensively [4-7]. When LPE epitaxially crystallizes on an iPP substrate the

zigzag LPE chains are at 50° angles to the *c*- axial direction of the iPP crystal lattice. This fact is often explained by the interaction of LPE chains with rows of methyl groups that are situated on the (010) plane of iPP α- crystals surfaces since LPE chains can fit well into valleys formed by the methyl groups of iPP [1- 13]. However, we know of only a few reports on the epitaxial growth of LPE on uniaxially oriented iPP [14-16].

Uniaxially oriented homopolymers including LPE or iPP, can show homoepitaxy, yielding structures called shish-kebabs [34]. An increased crystallization rate of LPE in the LPE/iPP blends has been attributed to the presence of various types of LPE nuclei surviving in the blend melt and the stabilizing action of the iPP crystal matrix [17].

Heterogeneous polymer epitaxial crystallization is not only significant theoretically but can also influence some important practical applications. In iPP/LPE blends increased tensile and impact properties have been observed [18]. Attention was focused also on mechanical properties [19-22], miscibility [23-25] and phase morphology [11]. It is expected to enhance the blend's mechanical properties through improvement of interfacial interaction since iPP/LPE blends are generally immiscible. Epitaxial growth can strengthen the interface due to close intermolecular interaction [26-28].

This contribution describes the structure and morphology of the homo- and heterogeneous epitaxialy nucleated blends. Unidirectionally oriented blends were prepared by continuous extrusion with elongational flow where the LPE phase was the matrix and 20, 30 or 40% of iPP, in the blend in the form of oriented fibrils, served as reinforcement of the LPE matrix [29].

EXPERIMENTAL PART

Materials

Table I lists the characteristics of the commercial samples of isotactic polypropylene and linear polyethylene used for blend preparation. The blends with 20, 30 and 40 % (w) of iPP were prepared by compounding using a counter rotating extruder at 35 rpm, temperature 190 - 210 °C and free cooling of the extrudate to room temperature. The blends, characterized by iPP fibrillar uniaxially oriented reinforcement embedded in the LPE matrix, were prepared by continuous extrusion at 170 °C with a semihyperbolic – converging die [29]. The ribbons, with cross-section 20 x 2 mm, were cooled free in the air at room temperature without further drawing or annealing.

Structure characterization

For sample structure and morphology characterization wide angle X-ray diffraction (WAXS), transmission electron microscopy (EM) and differential scanning calorimetry (DSC) were applied.

Wide – angle X-ray scattering. The X-ray diffraction sample scans were measured on an HZG diffractometer (Freiberg, Prazissionsmechanik, Germany) with a line shaped beam of CuK$_\alpha$ Ni-filtered radiation. Step size was 0.03° 2Θ and time 5s. Sample measurements were performed along and perpendicular to the extrusion direction (direction *a*, respectively *b*). Radial transmission scans were measured in the 2Θ interval 5 – 30 ° for 10 different location of each sample.

Sample crystallinity (X) was determined from the radial X-ray scans resolved for iPP and LPE contributions of the crystal and amorphous phases of both blend components using the procedure introduced by Weidinger and Hermans [30].

Crystal size (L_{110}) was calculated using the most intense crystal peaks (110), for both iPP and LPE, from the peak ½ width using the Scherrer equation [31]. As an "ideal" crystal the peak of phthalic acid at $2\Theta = 17.4°$ with ½ width 0,3° 2Θ was used.

Sample orientation based on X – ray diffraction could be measured by different methods [42]. Here we used the sample measurements in the directions along (*a*) and perpendicular (*b*) to the sample extrusion direction. The intensity ratio of 110 peaks *b/a* greater than 1 for either LPE or iPP indicates a preferred sample orientation for that polymer, similarly as the ratio I_{040}/I_{110} in iPP where this ratio grows from 0,65 to greater values in preferentially oriented samples [32 - 34].

The sample orientation degree of the iPP component (O_r) could also be characterized by the azimuthal angle where the 110 peak intensity decreased to ½; the smaller the values of O_r the greater the degree of orientation.

Electron microscopy

The sample morphology was characterized by transmission electron microscopy (TEM – Tesla BM 500, Tesla Brno, Czech Republic). The replicas of selectively etched sample surfaces were studied in detail. The procedure to create the first stage replicas was: 1. the surface of the extruded ribbon sample was selectively etched, 2. shadowed, 3. reinforced by evaporated C-layer, 4. replicated by polyvinylalcohol.

The sample etching was performed by a 1% solution of $KMnO_4$ in 85% H_3PO_4 at 25° C [35, 36]. The amorphous phase was etched first, but further etching of the crystal phase continued more in LPE than in iPP. The etching time was 10 min. Afterwards the samples were shadowed by a thin Au or Pt layer and reinforced by an evaporated C layer. For replication, a 10% water solution of polyvinylalcohol was used to remove the replica yielding a first stage replica. The magnification on TEM micrographs is shown by a 1μm bar. Replicas of the cryogenic fracture surfaces of extrudates were also observed.

Differential scanning calorimentry (DSC). The melting and crystallization behavior were followed under N_2 using a Perkin-Elmer Pyris-1 DSC (USA) calibrated by indium. The heating and cooling rate was 10 °C/min. The samples were heated to 220 °C for melting and cooled back for crystallization scans. The sample crystallinity was calculated from ΔH values assuming for iPP 209 J/g [35] and for LPE 293 J/g [36] for 100 % crystalline homopolymers.

RESULTS AND DISCUSSION

Figures 1a-e show typical radial X-ray diffraction scans of the ribbons of linear polyethylene (LPE, orthorhombic modification), isotactic polypropylene (iPP, α- modification) and their blends containing 20, 30 and 40% of iPP. No peaks of other crystal forms of iPP or LPE were detected. The crystallinity of both, homopolymers, extruded as described, was higher for LPE (59%) than for iPP (52%), which is normal, but the values were lower than in other samples oriented and annealed (55-63% in iPP [43], 87% in LPE [34]). The X-ray diffraction scans in the *a* and *b* extrusion directions represent a two-phase immiscible blend system with peaks of

iPP crystal planes 110, 040, 130, combined (111, 131, 041), 060 and 220 together with LPE 110 and 200 planes. The LPE 110 peak ($2\Theta \approx 21°$) intensity was increased by the coincident iPP peaks 111, 131 and 041. In LPE alone the peak intensities ratio 110/200 in a direction is 3.2 but in the blends with iPP it increases to 3.6 (Tab. II). The presence of the combine peaks (111, 131 and 041) on the equator scans means that the orientation of the iPP crystal c-axis in the extrusion direction is only partial. The total crystallinity values (X_t) measured in both a and b directions were practically identical within experimental errors (Table II), they were divided into individual LPE or iPP contributions according to initial blend composition (X_a values in Tab. II). Similar crystallinity results were obtained in the case when we modified the LPE 110 intensity by the iPP (111, 131 and 041) contribution. To divide the crystallinity values in the blends, for the total peak intensity of the combined peak at $2\Theta = 21°$ the iPP contribution was estimated as being equal to 0.68 I_{110} in scans a or 0.7 I_{110} in scans b (X_b values in Tab. II). The total sample blend crystallinity values of 52 - 60% were relatively low, indicating that the crystallization process was fast. X- ray diffraction scans of iPP or LPE alone showed no preferred orientation, the $b/a \approx$ 1 and I_{040}/I_{110} was close to 0.6 in iPP alone, but the iPP component in the blends showed preferred orientation according to the I_{110} b/a, I_{040}/I_{110} or O_r values. This situation is due to the fact that some longer lamellar branches were bent or tilted and their molecular axes have a different orientation than the molecules in the central line (discussed later).

The three strong equatorial reflections of iPP and the microscopical evidence (shown later) confirms that at least part of the c- molecular axes were preferentially oriented in the sample extrusion direction (a- measuring direction) (Figs. 1b-d) . This was confirmed by EM evidence

showing that some ribbons and long homo-epitaxial branches were oriented in different directions to the extrusion direction (see below, in Morphology).

The LPE alone and in the blends was randomly oriented because their intensity ratios, the I_b/I_a values, were close to 1. As is shown later, this was due to homoepitaxial branching where the amount of I_{110} was practically the same, the ratio b/a is close to 1 (Tab. II). The orientation degree of the blend may be characterized as a medium one. A higher orientation degree in the iPP / LPE blends could be achieved only by adapting the extrusion conditions individually for each blend or by orientation and annealing of the blends in separate procedures.

The 110 peak intensities of the iPP blend component measured at different azimuthal angles (Az) is shown in Fig. 2. From such plots the orientation degree, O_r, where the original peak intensity decreased to ½ was determined (ca 40°). Azimutal plots for the 040 iPP peak were similar.

The decreased intensity of I_{040} in the blends compared to the iPP alone shown in Fig. 1, indicates that the b- axis of the iPP crystals tended to be aligned perpendicular to the sample surface [39]. Generally, the results for 040 intensity measured in different directions (a,b) were slightly different due to crystal orientation. The blend crystallinities were close to the values of the non-oriented samples e.g. in [17, 21, 27]. The crystal sizes in the 110 direction (L_{110}) were lower both for iPP homopolymer (iPP 88 – 93 Å compared to LPE 152 – 132 Å) and also compared for annealed or unidirectionally oriented homopolymers (107 – 143 Å iPP [43], 281 – 294 Å LPE [34]). The L_{110} values of individual components in the blends were also lower with their decrease in the blend content. The orientation characteristic b/a of the iPP blend components changed from 1 (iPP alone) to 1,57 (for blend 40 % iPP/60 % LPE) or from 0.68 to 0,93 for the I_{040}/I_{110} ratio. In the blends the trend of the values b/a and I_{040}/I_{110} is similar in a direction. The b/a ratio

approaching to 1 means the sample's crystal orientation was random, which was true for LPE alone and as a blend component.

Melting and crystallization of iPP/LPE blends by DSC

The results of the melting and crystallization scans by DSC, summarized in Table III, confirmed that the blends of iPP/LPE represent generally an immiscible system with separate melting peaks of iPP ($T_m \sim$ 163 – 167 °C) and LPE ($T_m \sim$ 131 – 132 °C). After cooling the melt, the blend components crystallized individually: first iPP (T_c = 123,4 °C for the polymer alone and decreased for the blends with LPE) and later the LPE crystallizes (T_c = 114,7 °C for LPE alone and increased for blends with iPP). Both blend components crystallize in their own stable crystal structure, the iPP first, followed by LPE. The crystallization rate of LPE in the blend was faster (the crystallization temperature was higher) than that of LPE alone, which confirms the nucleation effect of the solid iPP crystals on the LPE crystallization. In addition to this nucleation action, there was a strong orientation effect of the oriented iPP fibrils forcing the LPE branches to grow inclined $\pm$ 50° to iPP fibril direction (shown in Figs 5 – 7). Partial mutual miscibility of both blend components led to a slight decrease of T_m and ΔH values of both components, compared to the individual polymers alone (Tab. III).

The crystallization temperatures, T_c, of iPP during cooling the melt were slightly decreased due to the LPE partially dissolved in the iPP. The crystallization temperature T_c of iPP in the blends decreased from 123.4 °C to 116 °C in the blend with 80% LPE. This is in accord with limited solubility of LPE in iPP.

The crystallization condition of LPE in the blend was different because it crystallized in the presence of already solid and oriented iPP fibrils. The LPE alone crystallized at $T_c = 114.7$ °C, but in the blends with iPP its crystallization temperature increased to ~ 116 °C, independently of the iPP amount in the blend. The solid iPP phase present in the LPE melts acted as nucleation sites for LPE crystallization and increased its crystallization rate and crystallization temperature. Melting during the second heating runs of crystallized samples resulted in slightly increased melting temperatures $T_{m(II)}$ of all samples. This confirms that the crystallization conditions in DSC measurements were more favorable than during original sample preparation. The comparison of crystallinity data based on DSC first run and X-ray diffraction measurements differed numerically by a few percent % in a favor of X-ray but the trend was similar.

Morphology

The crystal structure, orientation, melting and crystallization behavior of our samples was characterized above, electron microscopy complemented this information by providing examples of the local morphological structure. Typical electron micrographs of the extruded and selectively etched surfaces of iPP, LPE and their blends are shown in Figs. 3 – 9. Two types of epitaxial structures were clearly visible: homoepitaxy and heteroepitaxy. Both homopolymers, LPE or iPP, (Figs. 3 or 4) were characterized by bands (shish-kebabs) oriented in the extrusion direction with a narrow central line (the shish, C) and dense side branches initially oriented perpendicular to the central line (the kebab). In the LPE sample (Fig. 3) the shishs were ~300 Å thick, individual and relatively far apart (0,6 -1 μm) with dense perpendicular branches (kebab)

300 - 500 Å thick and about 1 µm long with a tendency to undulate. In some places the branches were bent, inclined and randomly organized independent of the shish.

In iPP the central lines tended to form parallel bunches of 2 – 3 lines lying close together (Fig. 4). The sets of parallel bunches were 2 – 3 µm apart which was more than in LPE. The iPP shishs were fully covered by short perpendicular lamellae, 1000 – 1500 Å long and 200 – 400 Å thick. Where the neighbouring shishs were further apart, long branches were also seen, the length of the long branches increasing up to about 2 – 3 µm. In some places the lamellae grew independently of the central line position, without preferred orientation. The short branches of iPP (marked by sb) were straight without undulation. The long iPP branches (lb) have a tendency to show further secondary branching, similar to cross-hatched spherulitic structure (S) [40 – 41].

Figure 5, of the 20/80 % iPP/LPE blend, shows parts with homoepitaxy of iPP (Ho) and parts with the LPE heteroepitaxy (He) in form of lamellar branches inclined ± 50° to the iPP extended shish. The LPE branches, 300 -500 Å thick and up to 1µm long, are mostly straight or slightly bent without the undulation tendency seen in LPE alone. The prevailing sample surface was covered by stacks of LPE lamellar branches. The iPP central lines tended to lay closely parallel to each other, leaving more space to LPE material. In some locations (F) the long LPE lamellae seem not to be attached to iPP.

In Figs. 6 and 7, of blends with 30 or 40% of iPP, the LPE overgrowth is similar as in the sample 20/80 (Fig. 5). Figure 6 shows a few locations where small globular (G), lamellar (L) and cross-hatched (C) formation, supposedly LPE phase, grew independently of the iPP oriented rows. The central lines of iPP show again the tendency being close together leaving more space for LPE overgrowth (Fig. 7).

Figure 8 of the etched cryogenic fracture surface of the 40/60 blend shows oval fibrils of iPP broken mostly perpendicular to the extrusion direction. The oval dark structures are shish cross-sections (Fig. 8).The fracture surface shows that the fibrils, consisted of presumably of closely spaced shishs of components assembled side by side. The components were band's cross-sections oriented along the extrusion direction; their cross-section was characterized by apparent lamellae with thickness of 200 – 400 Å and lateral size up to 0,5 μm.

Figure 9 shows the fracture surface of the sample iPP/LPE 40/60 fractured along the extrusion direction. The fracture surface of the inside of the fibrils (R) was characterized by lamellae oriented along the extrusion direction, the ribbon surface was covered by short iPP branches (Sb) or by thicker LPE overgrowth (B) inclined to the sample extrusion direction. The bands thickness in Fig.9 in extrusion direction is similar to that in Figs. 6 and 7 as well as the LPE overgrowth orientation.

As shown by the EM images, the samples represent a two-phase mostly immiscible blend system, where, in the LPE matrix, the parallel oriented iPP fibrils were covered by epitaxially attached LPE branches in the form of lamellae inclined ca ± 50° to the sample extension direction. The iPP fibrils were generally straight or slightly bent, their diameter varied between 0.2 – 3 μm (Fig.8) and the fibril cross-sections were elliptical. The LPE branches were chain folded lamellae, their length varied according to available lateral space and their thickness was in the range 300 – 500 Å. The longer branches tended to bend and incline. The extended iPP fibrils consisted of α- modification crystals of isotactic iPP, mostly oriented with their c- crystal axes parallel with the sample extrusion direction. The iPP fibrils were densely covered by short (1000 - 1500 Å) perpendicular iPP branches or longer branches. The LPE in the pure polymer consisted

of long oriented central lines (shish) and perpendicular branches, short or longer according to available space. The perpendicular branches tended to bend and tilt as they grow. In blends with iPP the LPE bands were oriented approximately ± 50°to the oriented iPP central shishs.

CONCLUSIONS

The epitaxial crystallization of melt oriented iPP/LPE blends yielded two types of epitaxial structures: 1) homoepitaxy of both components where the branches, shorter in iPP and longer in LPE, are initially oriented perpendicular to extrusion direction and 2) heteroepitaxy of LPE on initially crystallized iPP fibrils. The positive mutual interaction of iPP and LPE was confirmed by the fact that solid iPP represents a heterogeneous nucleation surface for LPE crystallization such that its lamellae are inclined ± 50° to the extension direction. Partial limited mutual solubility of both blend components influences the crystallization and melting behavior of the blend.

The blend extrusion process led to a structure of the iPP phase slightly oriented in the extrusion direction. The relative short crystallization time resulted in a higher amorphous content and lower crystallinity, crystal size and melting temperatures than in other higly oriented or annealed samples of iPP or LPE.

Acknowledgement

ACCEPTED MANUSCRIPT

List of references

[1] J. WILLEMS. Oriented growth in the field of organic high polymers. *Discuss. Faraday. Soc.* 1958, 23, 111-113

[2] E.W. FISHER. Orientierte Kristallisation des Polyethylens auf Steinsalz, *Kolloid-* Z. 1958, 159, 108

[3] S.W. WELLINGHOFF, F.RYBNIKAR and E.BAER. Epitaxial Crystallization of Polyethylene. *J.Macromol.Sci., Part B.,Phys.* 1974, B10, 1-39

[4] J.C. WITTMANN and B.LOTZ., Epitaxial crystallization of polyethylene on organic substrates – A reappraisal of the mode of action of selected nucleating-agents, *J.Macromol.Sci., Part B.,Phys.* 1981, B19, 1837-1851.

[5] A.J.LOVINGER and M.L.WILLIAMS. Tensile properties and morphology of blends of polyethylene and polypropylene, *J.Appl. Polym.Sci.* 1980, 25, 1703-1713.

[6] J.C. WITTMANN, A.M. HODGE and B.LOTZ., Epitaxial crystallization of polymers onto benzoic-acid – polyethylene and paraffins, aliphatic polyesters and polyamides, *J.Polym.Sci.-Polym.Phys.* 1983, 21, 2495-2509.

[7] W.P.ZHANG and D.I.DORSET., Epitaxial growth of long-chain molecules on potassium hydrogen phthalate and potassium-chloride substrates from the vapor-phase, *J.Polym.Sci.-Polym.Phys.* 1989, 27, 1433-1447.

[8] J.WANG, A.KAITO, S.OHNISHI, N.TANIGAKI and K.YASE., Temperature effect on epitaxial growth of poly(p-oxybenzoate), *J.Macromol.Sci., Part B.,Phys.*. 1998, B37, 1-13.

[9] S.K., YAN, J.LIN, D.YANG, J. PETERMAN. Critical epitaxial layer of different kinds of polyethylene on highly oriented isotactic poly(propylene) substrates, *Macromol. Chem. Phys*. 1994, 195, 195-201.

[10] B.GROSS, and J.PETERMAN. Synergism of mechanical-properties in blends of semi-crystalline polymers, *J.Mater.Sci*. 1984, 19, 105-112.

[11] M.KOJIMA, and H.SATAKE. Morphological and structural features of heat-treated drawn polypropylene high-density polyethylene blends, *J.Polym.Sci.-Polym.Phys*. 1984, 22, 285-294.

[12] J. PETERMAN, G.BROZA, G.RIECK, A. KAWAGUCHI, Epitaxial interfaces in semicrystalline polymers and their applications, *J.Mater.Sci.* 1987, 22, 1477-1481.

[13] B.LOTZ and J.C. WITTMANN. Structural relationship in blends of isotactic polypropylene and polymers with aliphatic sequences, *J.Polym.Sci. Part B*. 1986, 24, 1559- 1575.

[14] R. SU, Z. LI, H. BAI, K. WANG, Q. ZHANG, Q. FU, Z. ZHANG, Y. MEN, Flow-induced epitaxial growth of high density polyethylene in its blends with low crystallizable polypropylene copolymer, *Polymer.* 2011, 52, 3655-3660.

[15] G.ZERBI, H.CIAMPELLI and V.ZAMBONI. Classification of crystallinity bands in infrared spectra of polymers, *J.Polym. Sci.,* 1963, C7, 141- 151.

[16] H.N AN, B.J. Zhao, Z. Ma, C.G. Shao, X. Wang, Y.P.Fang, L.B. Li, Z.M. Li, Shear-induced conformational ordering in the melt of isotactic polypropylene, *Macromolecules.* 2007, 40, 4740-4743.

[17] F.RYBNIKAR. Crystallization and morphology in blends of isotactic polypropylene and linear polyethylene. *J.Macromol.Sci., Part B.,Phys.* 1988, B27, 125-144

[18] R.H.OLLEY, A. M. HODGE, D. C. BASSETT, A permanganic etchant for polyolefines *J. Polym. Sci. Polym.Phys Ed.* 1979, 17, 627-643.

[19] K.WANG, S.LIANG, R.N.DU, Q.ZHANG and Q.FU., The interplay of thermodynamics and shear on the dispersion of polymer nanocomposite, *Polymer.* 2004, 45, 7953-7960.

[20] R.H. OLLEY, and D.C. BASSETT, An Improved Permanganic Etchant For Polyolefines *Polymer.* 1982, 3, 1707-1710.

[21] Z.BARTCZAK, A.GALESKI and M.PRACELLA¸ Spherulite nucleation in blends of isotactic polypropylene with high-density polyethylene, *Polymer.* 1986, 27, 537-543.

[22] C.SIVESTRE, S.CIMMINO and B.PIROZZI, Morphology of a melt crystallized iPP/HDPE/hydrogenated hydrocarbon resin blend, *Polymer.* 2003, 44, 4273-4281.

[23] Y.J. LIN, G.R. MARCHAND, A. HILTNER and E. BAER. Adhesion of olefin block copolymers to polypropylene and high density polyethylene and their effectiveness as compatibilizers in blends, *Polymer.* 2011, 52, 1635-1645.

[24] E. NOLLEY, J.W. BARLOW and D.R. PAUL. Mechanical properties of polypropylene-low density polyethylene blends, *Polym. Eng. Sci.* 1980, 20, 364-369.

[25] W.N. KIM, S.I. HONG, J.S. CHOI and K.H. LEE., Morphology and mechanical properties of biaxially oriented films of polypropylene and HDPE blends, *J. Appl.Polym. Sci.* 1994, 54, 1741-1750.

[26] N. BING, K.WANG, P. ZHAO, Q. ZHANG, R. DU, Q. FU, Z. YU, E. CHEN, Epitaxy growth and directed crystallization of high-density polyethylene in the oriented blends with isotactic polypropylene, *Polymer.* 2005, 6, 5258-5267.

[27] B. GROSS and J. PETERMAN, Synergisms of mechanical properties of semicrystalline polymers, *J. Mater. Sci*. 1984, 19, 105-112.

[28] P. SCHMIDT, J. BALDRIAN, J. SCUDLA, J. DYBAL, M. RAAB, K.-J. EICHHORN, Structural transformation of polyethylene phase in oriented polyethylene/polypropylene blends: a hierarchical structure approach, *Polymer.* 2001, 42, 5321-5326.

[29] M.POLASKOVA, R. CERMAK, T. SEDLACEK, J. KALUS, M. OBADAL, P. SAHA, Extrusion of Polyethylene/Polypropylene Blends with Microfibrillar-Phase Morphology*, Polymer Composites.* 2010, 42, 1427-1433.

[30] WEIDINGER and P.H.HERMANS, On the determination of the crystalline fraction of isotactic polypropylene from X-ray diffraction, *Die Makromolekulare Chemie,* 1961, 50, 98-115

[31] P. SCHERRER, (1918) Bestimmung der Grosse und der inneren Struktur von Kolloidteilchen mittels Rontgenstrahlen. In: ALEXANDER, L. E.; X-Ray Diffraction Methods in Polymer Science. New York : Wiley-Interscience, (1969). p. 582

[32] F. RYBNIKAR, Orientation in composite of polypropylene and talc, *J.Appl. Polym.Sci.* 1989, 38, 1479-1490

[33] CH. WOO JIN and K. SUNG CHUL. Effects of talc orientation and non-isothermal crystallization rate on crystal orientation of polypropylene in injection-molded polypropylene/ethylene–propylene rubber/talc blends, *Polymer.* 2004, 45, 2393-2401

[34] F. RYBNIKAR, M. KASZONYIOVA, R. CERMAK, V. HABROVA, M. OBADAL, Structure and morphology of linear polyethylene extrudates induced by elongational flow, *J. Applied Polym. Sci.,* 2013, 128, 1665-1672

[35] F. RYBNIKAR, Selective etching of polyolefines II. Isotactic polypropylene, linear and branched polyethylene. In. B.Sedlacek: Morphology of polymers, (1986), Walter de Gruiter Co. Berlin – New York.

[36] F. RYBNIKAR, Selective etching of polyolefines I. Isotactic polypropylene, *J. Appl. Polym. Sci.* 1985, 30, 1949-1961

[37] K. MEZGHANI and P.J. PHILLIPS, The γ phase of high molecular weight isotactic polypropylene: III. The equilibrium melting point and the phase diagram, *Polymer* (1998), 39, 3735-3744

[38] V.B.F. MATHOT and M.F.J.PIJPERS. The heat capacity, enthalpy and crystallinity from DSC measurements and determination of the DSC peak base line. *Thermochimica Acta.* (1989), 151, 241-259.

[39] M.C.BRANCIFORTI, C. A. OLIVEIRA, J.A. de SOUSA, Molecular orientation, crystallinity, and flexural modulus correlations in injection molded polypropylene/talc composites, *Polymer Adv. Technol.* (2010), 21, 322-330

[40] B.LOTZ and C.J. WITTMANN, The molecular origin of lamellar branching in the alpha(monoclinic) form of isotactic polypropylene, *J. Polym. Sci. Polymer Phys.* (1986), Vol. 24, p. 1541-1558

[41] J.J. ZHOU, J.G. LIU, S.K. YAN, J.Y. DONG, L. LI, C.M. CHAN, J. M. SCHULTZ, Atomic force microscopy study of the lamellar growth of isotactic polypropylene, *Polymer* 46, (2005), p. 4077-4087

[42] L.E. ALEXANDER; X-Ray Diffraction Methods in Polymer Science. New York: Wiley-Interscience, 1969.

ACCEPTED MANUSCRIPT

[43] M. KASZONYIOVA, F. RYBNIKAR, J. KUCERA, J. SADILEK, Annealing of uniaxially oriented isotactic polypropylene, *Chemicke listy*, In press.

List of figures

Fig. 1 a - e. WAXS scans of iPP(a), LPE (b) and 20/80(c), 30/70(d) and 40/60(e) iPP/LPE blends in *a* and *b* sample extrusion direction. The underlined indices indicate LPE diffraction peaks. Fig. 1a – The combine peaks (111, 131, 041) in the iPP radial scans means that the iPP crystals are not fully oriented in the extrusion direction. In the scans of iPP/LPE blends the iPP contribution to the LPE 110 peak intensities reflects the increased 110/200 ration (Tab. II). Fig.1e – Dashed is shown as an example the iPP contribution in the 110 LPE peak intensity ($2\theta \approx 21°$) applied in calculation of X_b in Tab.II.

Fig. 1a, 100% PP
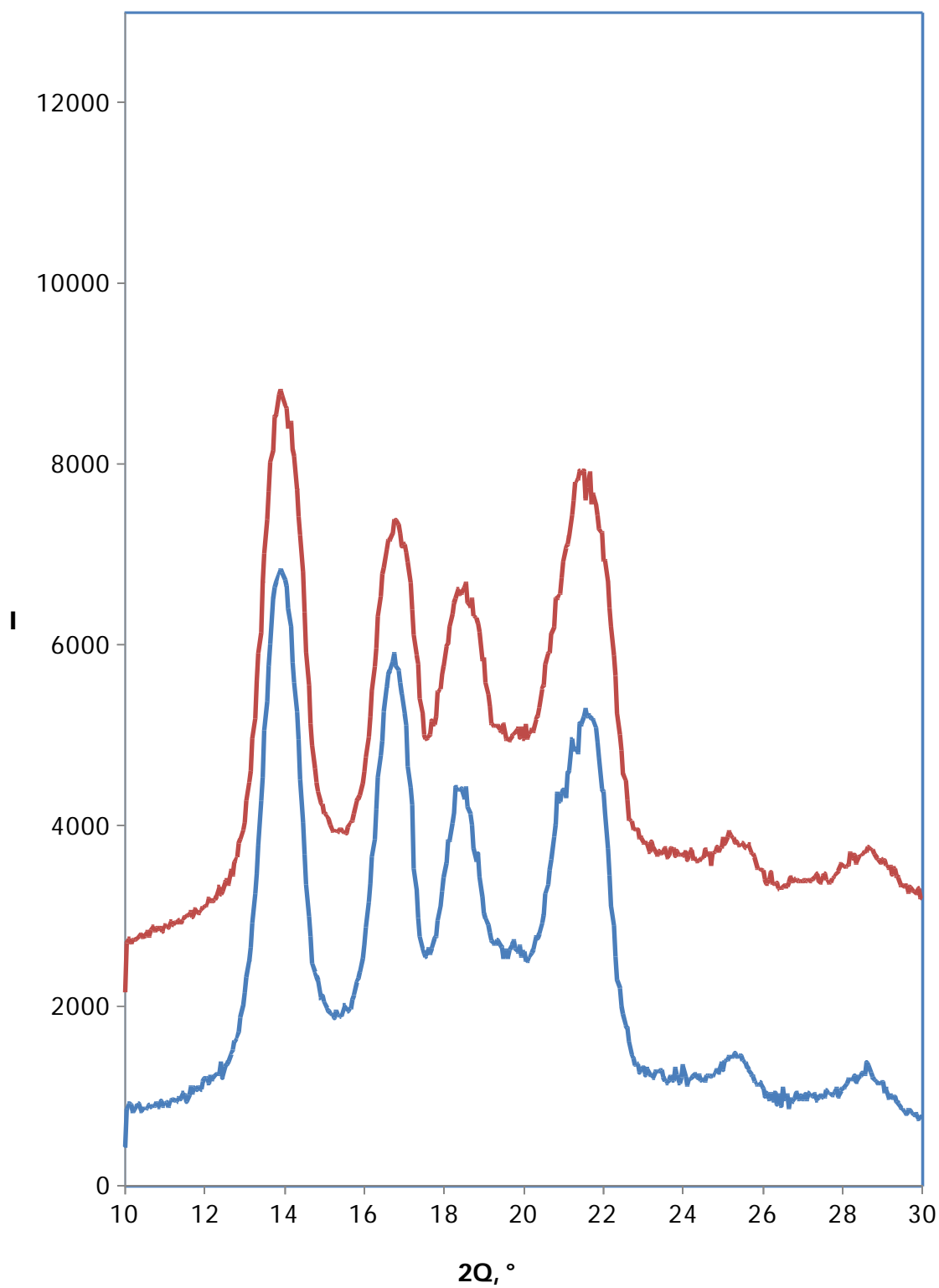
Fig. 1b, 100% PE
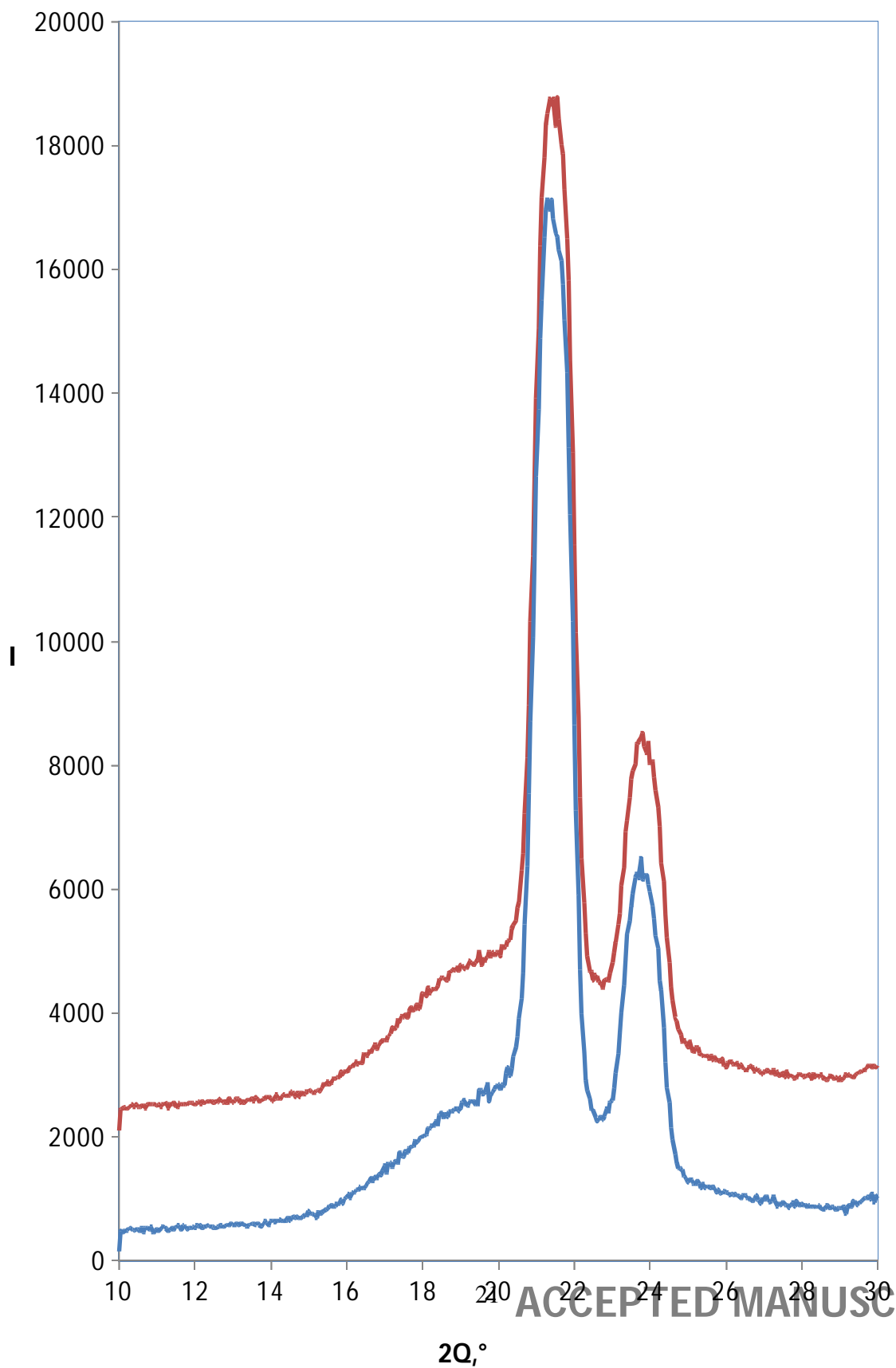
Fig. 1c 20% PP

Fig. 1d, 30%PP

I

2Q,°
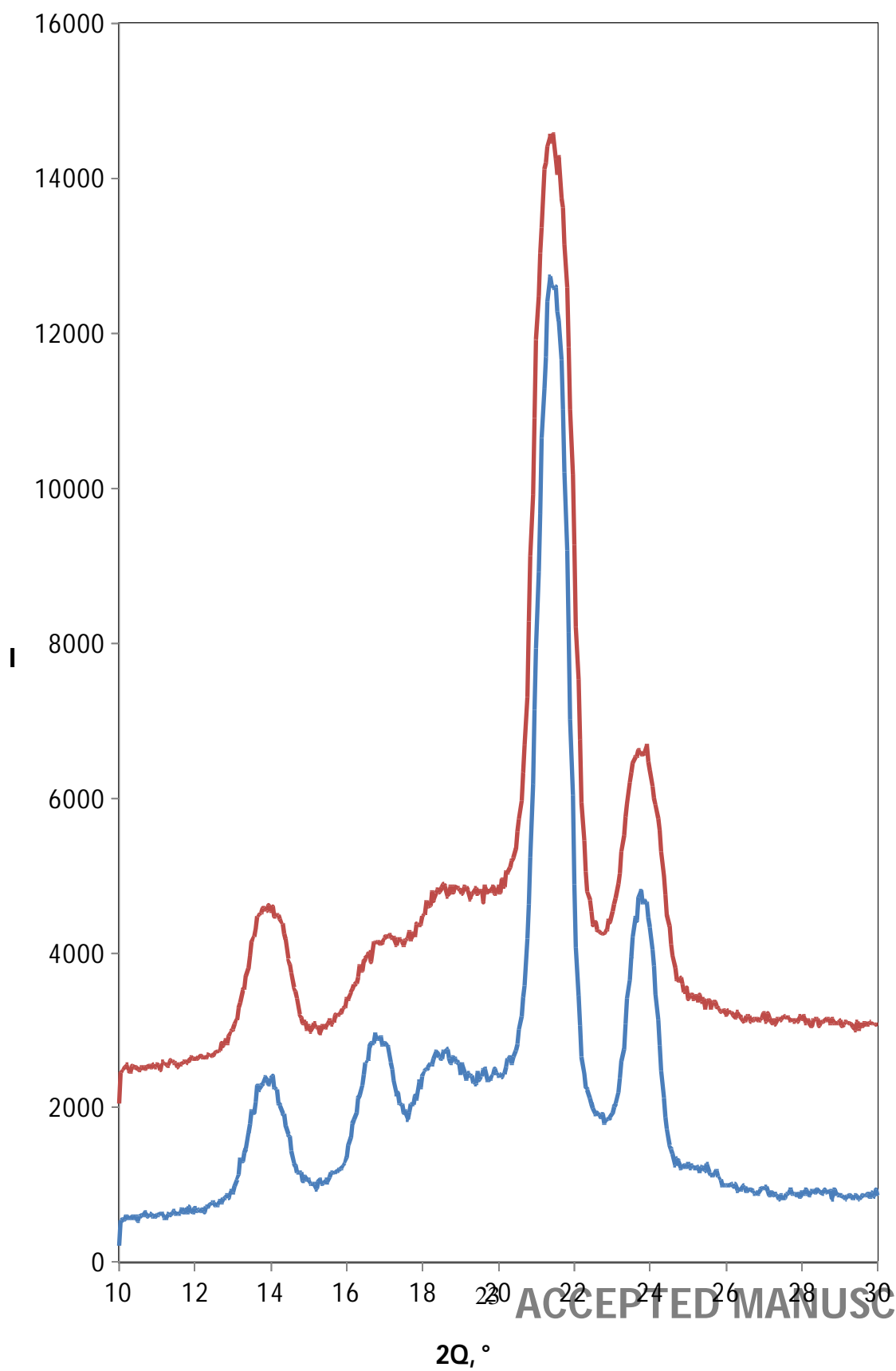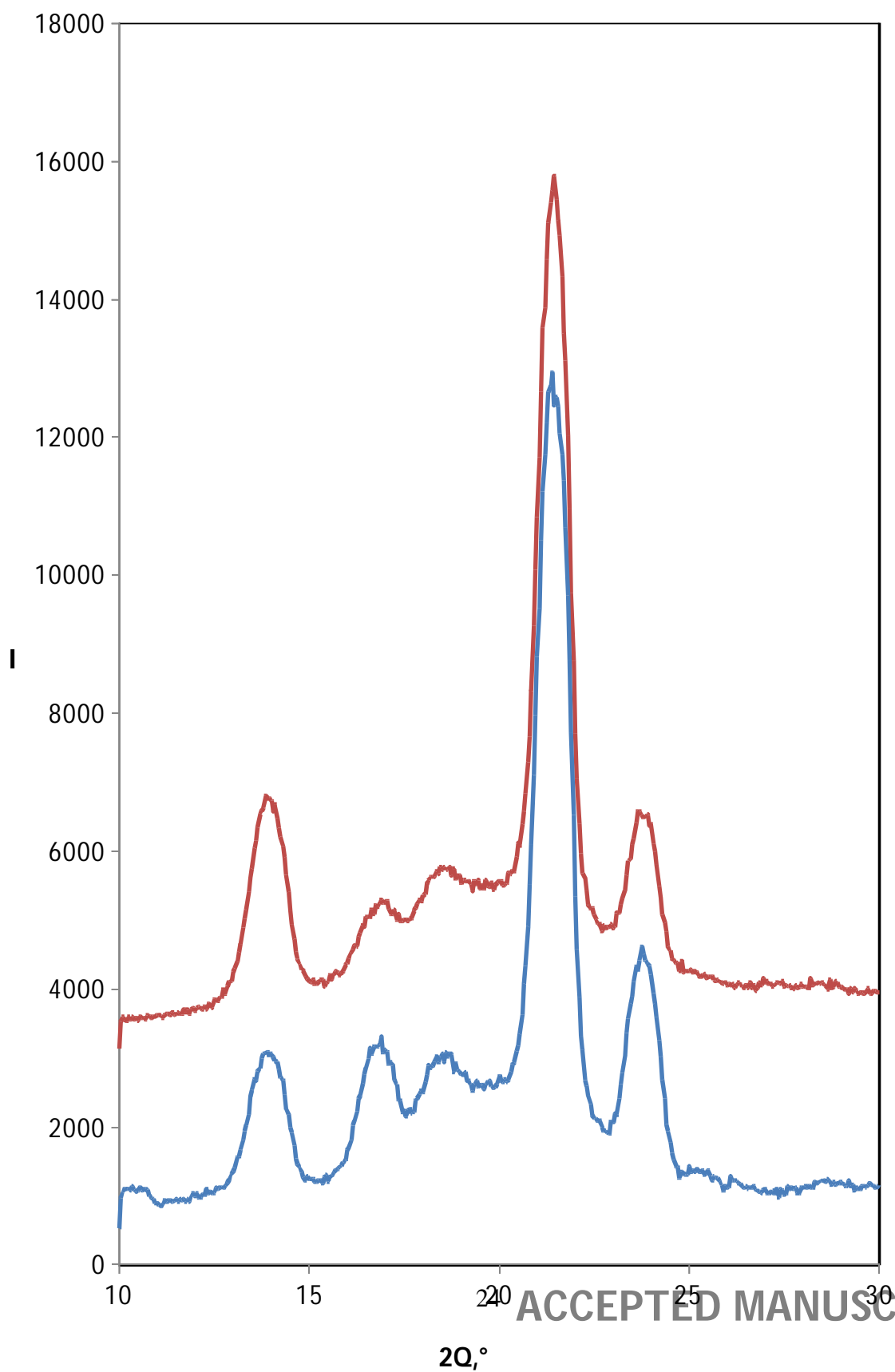
Fig. 1e 40% PP
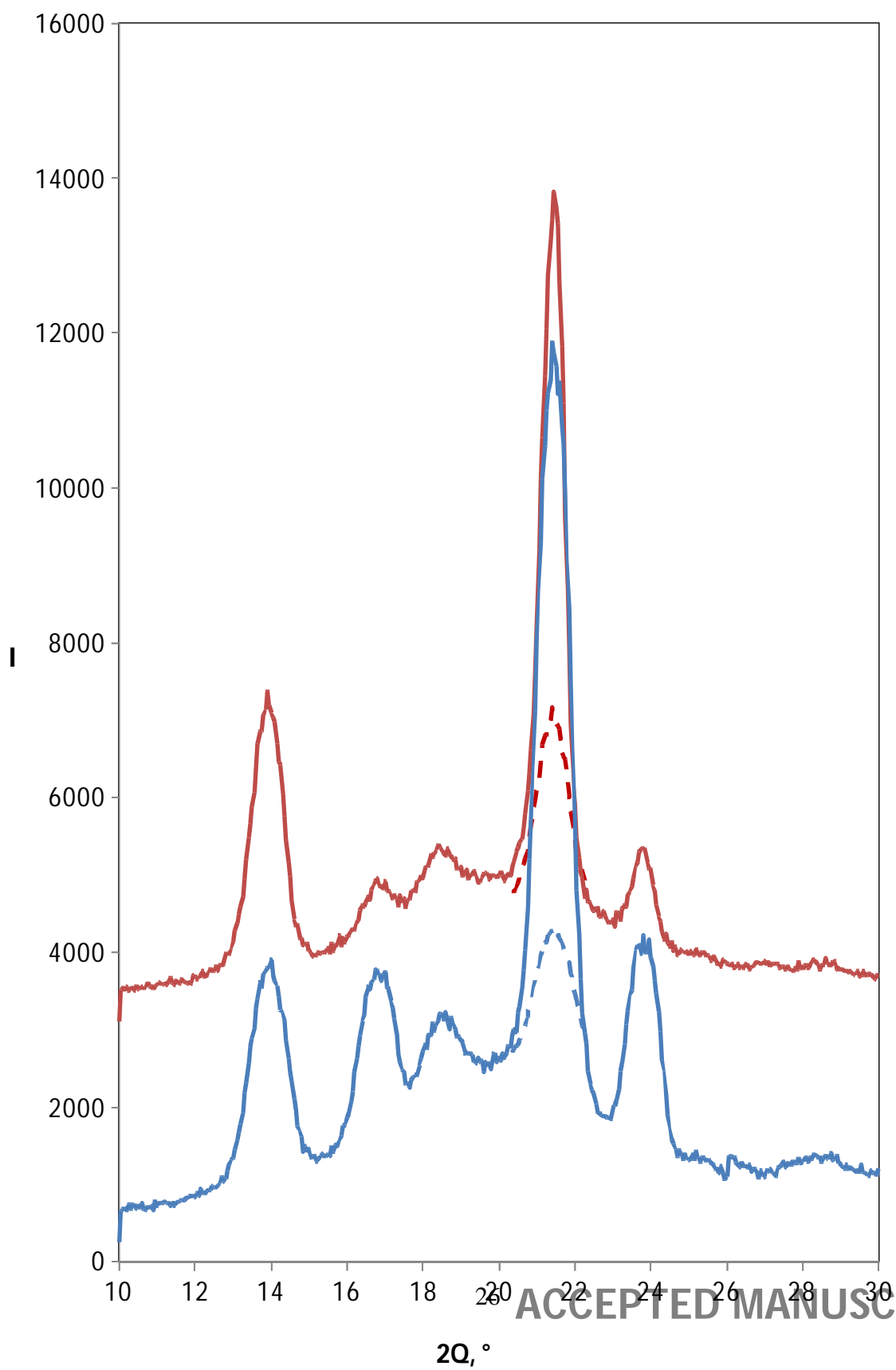
Fig. 2 The peak 110 intensity of the iPP component in the blends with lPE measured at different

azimuthal angles (Az).

ACCEPTED MANUSCRIPT

Fig.2
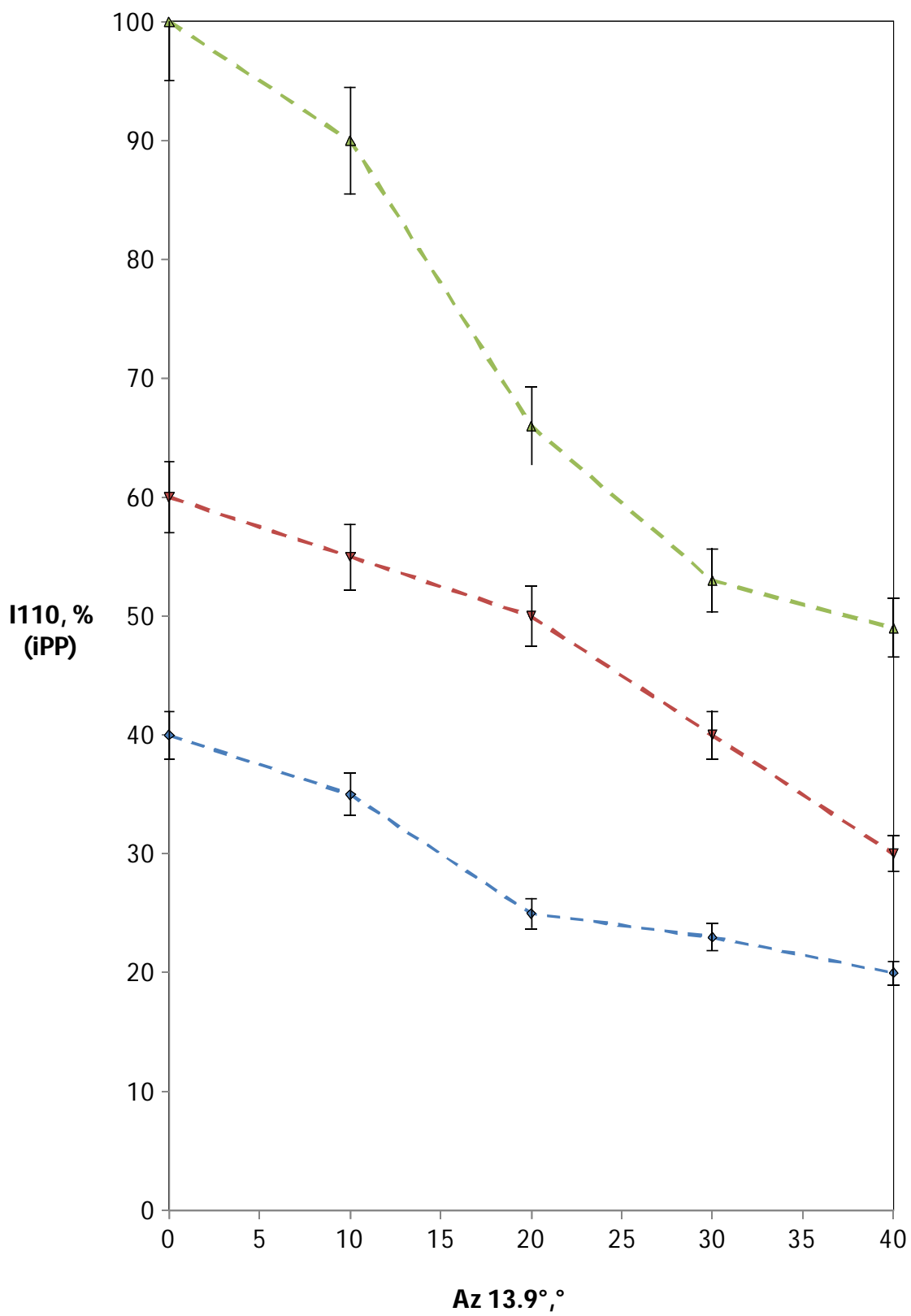
Fig. 3 Electron micrograph of the selectively etched surface replica of the linear polyethylene. The sample extrusion direction is marked by an arrow (↑). Central line (marker by C) represents the extended polyethylene chains. The lateral distance of individual extended parallel sish means that their concentration is relatively low. The undulating lamellae oriented ≈ 90° to the central line represent the homoepitaxial LPE kebab's overgrowth.
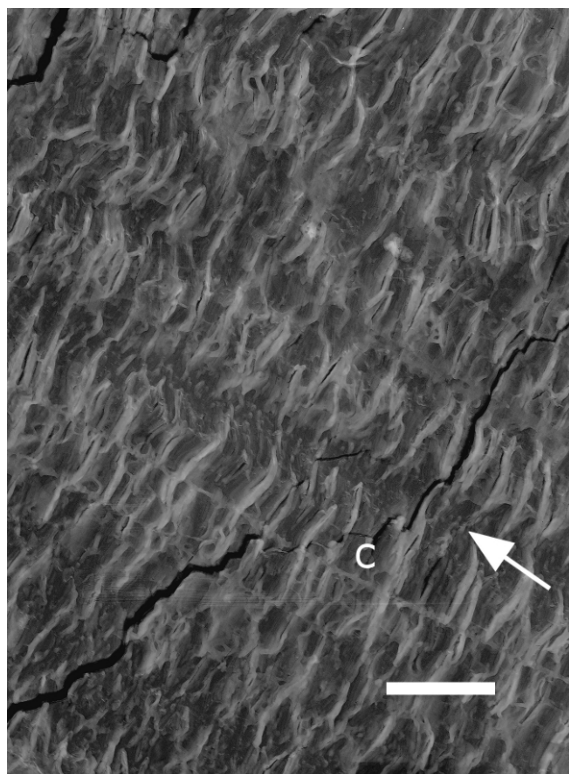

Fig. 4 Electron micrograph of the selectively etched surface of iPP. The multiple central line oriented in extrusion direction is covered by short perpendicular lamellae (sb) that can further

grow to longer branches (lb) slightly curved. Long branches can further branch by short perpendicular branches similar as seen in crosshatched spherulites [40-41]. Here this tendency is marked by (S). Next to chain extended in the extrusion direction there is ample space to less oriented branches or free lamellar formations.
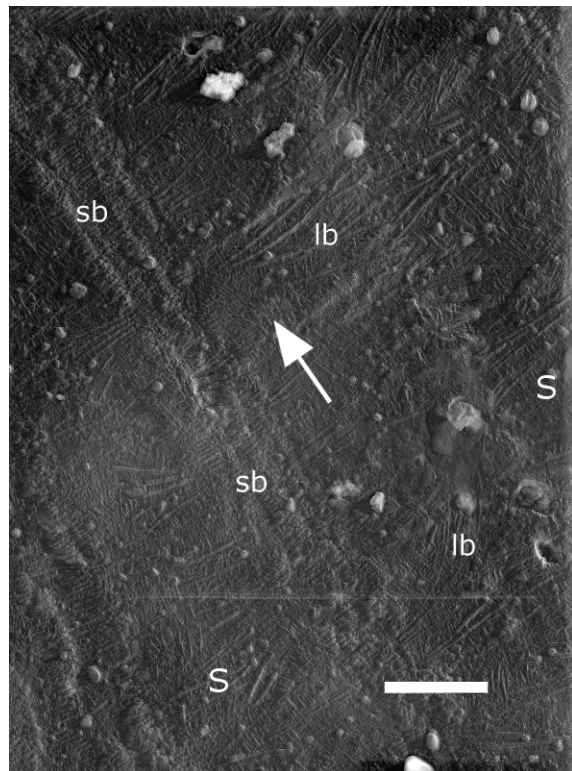

Fig. 5 Electron micrograph of the replica of the selectively etched surface of the blend 20/80. Both homo- (Ho) and hetero- (He) epitaxy of iPP and LPE forms are visible. Long LPE lamellae seem not to be attached to the shishs (F). The concentration of central lines or their parallel clusters oriented in the extrusion direction is relatively low.
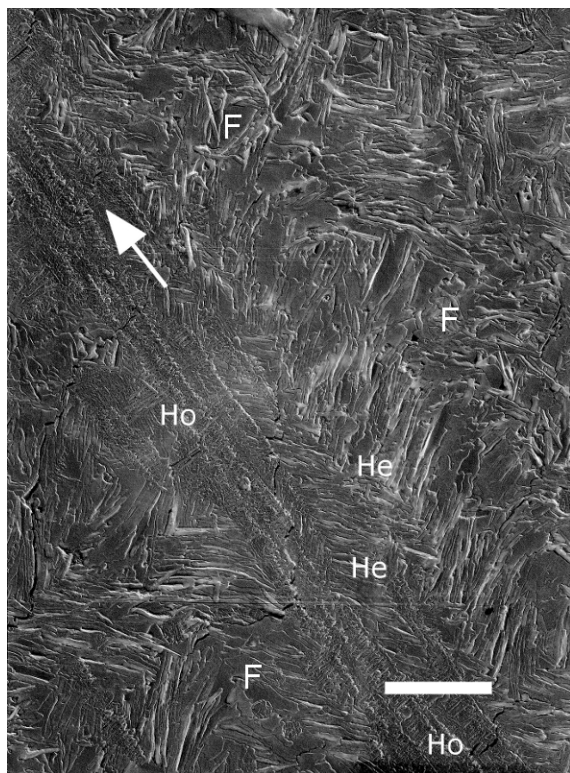
Fig. 6 Electron micrograph of the replica of a selectively etched surface, blend 30/70. The iPP ribbons with the thick LPE overgrowth are 0,4 – 0,6 µm wide. In addition globular (G) or short lamellar (L) isolated LPE formation appear independently on iPP ribbons. In some places the iPP tends to form cross-hatched structures (C). The central lines supposed in the centre of parallel bands are seen only rarely, because they are covered by a dense LPE overgrowth.

ACCEPTED MANUSCRIPT
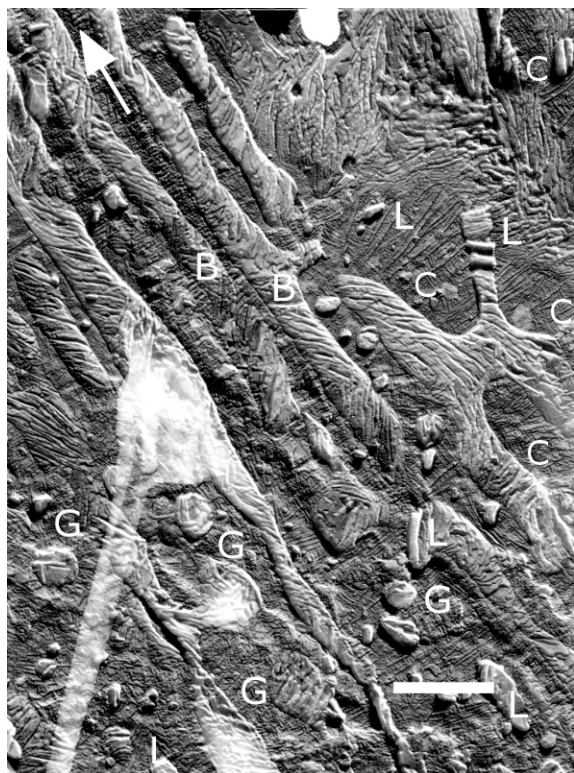
Fig. 7 Electron micrograph of the replica of selectively etched surface of sample blend 40/60. The homoepitaxy of iPP and heteroepitaxy of LPE on iPP is apparent. Both in Fig. 6. and 7 the central iPP line bunches are closer together than in Fig. 4 or 5 because of a higher iPP concentration in the band.
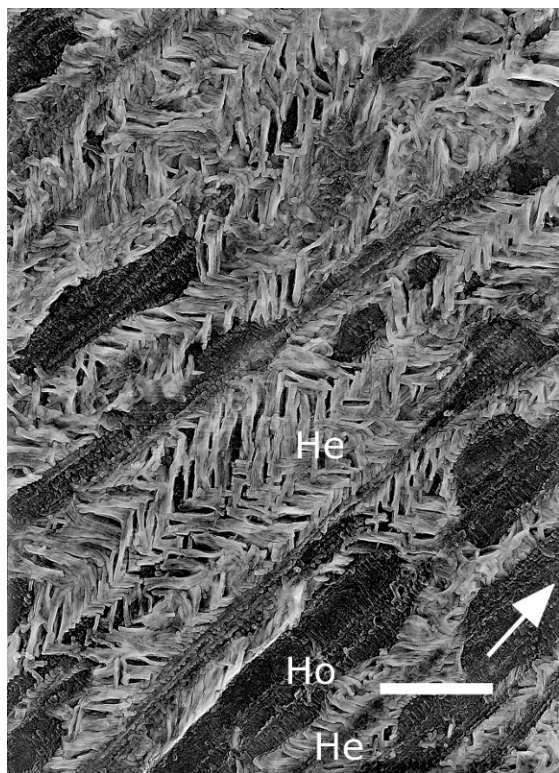
Fig. 8 Electron micrograph of the selectively etched fracture surface of the 40/60 iPP/LPE blend.

The sample was fractured perpendicular to the extrusion direction. Oval fibrils cross-section (0,2 – 2 μm) of iPP phase are covered by LPE matrix. Inset shows detailed structure of a ribbon.
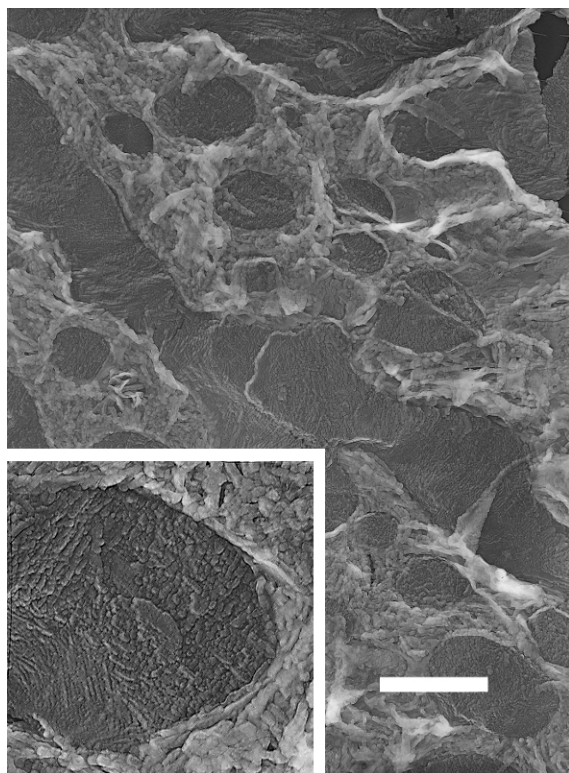
Fig. 9 Electron micrograph of a similar selectively etched fracture sample of 40 /60 iPP/LPE blend. The sample was fractured along the extrusion direction (↑). The structure of the ribbon oriented along the extrusion direction in the inner part (R) and on the surface covered by iPP short branches (Sb) or inclined LPE branches (B) are visible.

34
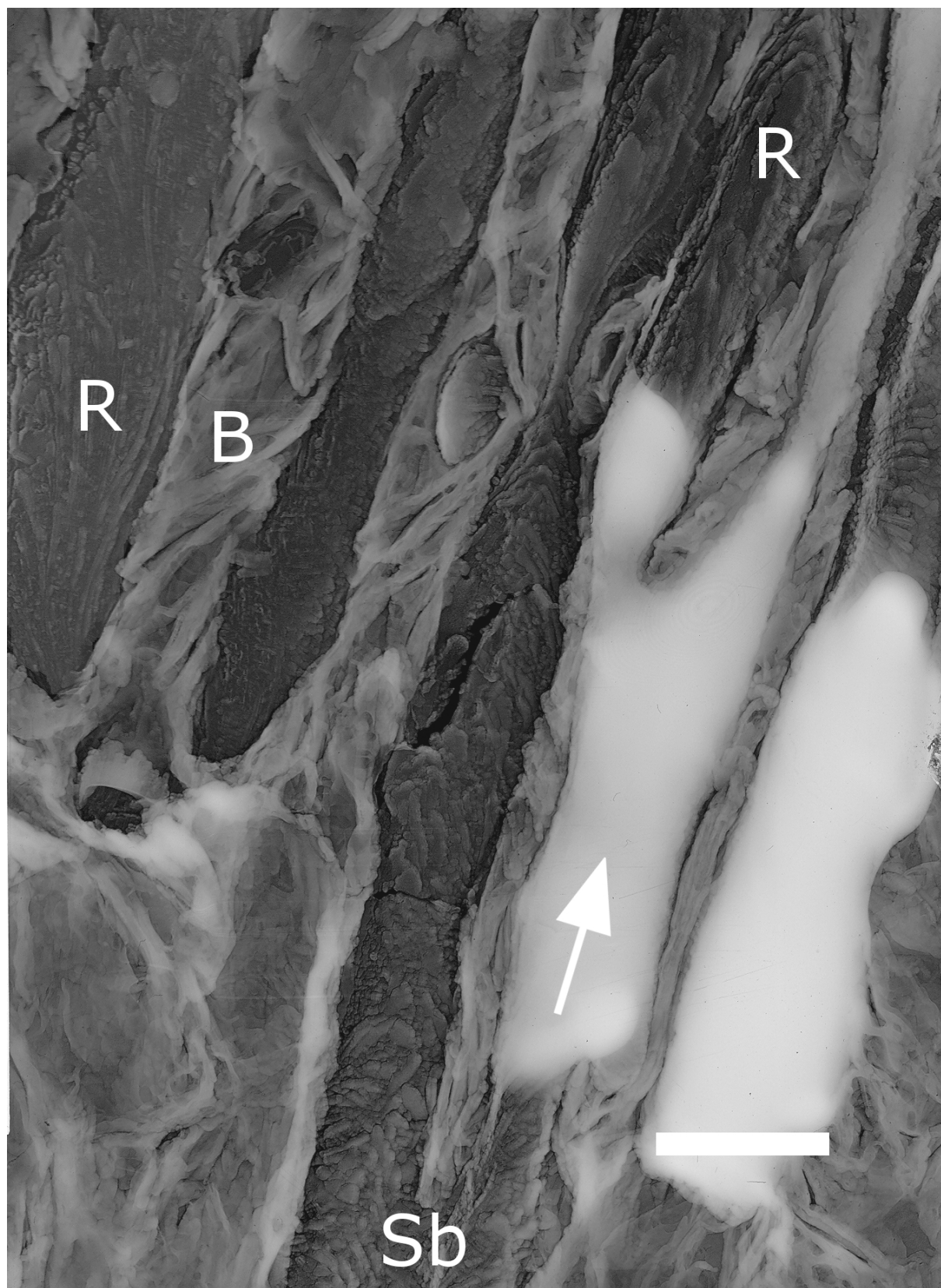
List of tables

I Sample characteristics

Tab. I Characteristics of linear polyethylene and isotactic polypropylene samples.

Sample	MFI, g/10min (ISO 1133)	M.W., 10^3, by GPC	Density, g/cm^3	Isotactic index, %, ISO 9113
iPP	3.2	360	0.91	98
LPE	0.55	140	0.95	

MFI - melt flow index, ISO 1133

M.W. - number awerage molecular weight by gel premation chromatography

II Results of X-ray diffraction analysis of iPP/LPE blends

Tab II. X-ray diffraction characterization of structure and orientation of iPP/LPE blends

iPP/LPE, %	M.D.	%X_t	%A	%X_a		%X_b		L_{110}, Å		I_{110}, b/a		I_{040}/I_{110}	Or, ° 110 iPP ±3°	$I_{110/200}$ LPE
				iPP	LPE	iPP	LPE	iPP	LPE	iPP	LPE	iPP		
20/80	a	57	43	11.4	45.6	15.2	41.6	63	134	1.30	1.10	0.90	40	3-Mar
	b	54	46	10.8	43.2	14.0	40.0	67	128			0.31		3-Aug
30/70	a	60	40	18.0	42.0	19.3	40.7	94	124	1.50	1.16	0.8	40	3-May
	b	56	44	16.8	39.2	21.3	34.6	103	139			0.28		5-Mar

40/60	a	55	46	22.0	33.0	21.3	33.6	100	124	1.57	0.96	0.8	40	3-Jun
	b	54	48	21.6	32.4	26.4	27.6	106	127			0.31		7-May
100/0	a	52	48	52.0				88		1.00		0.68		
	b	52	48	52.0				93				0.63		
0/100	a	59	42		59.0				152		1.00			3-Feb
	b	57	44		57.0				132					3-Apr

MD - measuring direction, a - along, b - perpendicular to extrusion direction

X_t - total crystalline phase; A - total amorphous phase; X_a - part of X_t derived according to blend composition;

X_b - this values were calculated assuming that the combined peak 2Θ - 21°intensity correspond for iPP 0.6 x I_{110} in scans <u>a</u> and 0.7 x I_{110} in scans <u>b</u>.

L_{110} - crystal size in 110 direction; I_{040}/I_{110} - orientation characteristic; O_r- orientation degree $I_{0.5}$

$I_{110/200}$ LPE - the ratio of two peaks 110/200 of linear LPE

III Results of melting and crystallization of iPP/LPE blends measured by DSC

Tab. III Melting and crystallization of iPP/LPE blends by DSC

%i PP in blend	$T_{m(I)}$, °C	ΔH J/g	% X (DSC)	T_c, °C	ΔH J/g	%X	$T_{m(II)}$, °C	ΔH J/g	$\%X_{DSC}$	$\%X_{X-ray}$
20	162.7	17.8	8.5	116	17.2	8.5	162.8	17.3	8.5	11-Jun
30	162.5	26	12.4	122.5	26	12.4	163	26	12.4	17.4

| 40 | 162.8 | 36 | 17.2 | 121.9 | 36 | 17.2 | 164.7 | 36 | 17.2 | 21-Aug |
| 100 | 164.8 | 113 | 54 | 123.4 | 108.3 | 52 | 166.7 | 113 | 54 | 52 |

ΔH 100% iPP = 209 J/g

%LPE in blend

60	130.5	106.3	39	116.5	152.2	52	131.8	110.4	37.7	32.7
70	129.4	124.5	45	116	161.8	55	131.1	133	45.3	40.6
80	129.9	144.7	52	116.5	152.2	59	131.4	152	51.9	44.4
100	132.6	189.3	66	114.7	191	65	132	184.2	66	58

ΔH 100% LPE = 293 j/g

$T_{m(II)}$ - second run melting